

Intramolecular Excitation Energy Transfer in Bichromophoric Compounds in Stretched Polymer Films

Miki Hasegawa,[†] Shigendo Enomoto,[†] Toshihiko Hoshi,[†] Katsuyuki Igarashi,[‡]
Tomoko Yamazaki,[‡] Yoshinobu Nishimura,[‡] Shammai Speiser,[§] and Iwao Yamazaki^{*,‡}

College of Science and Engineering, Aoyama Gakuin University, Chitosedai, Setagaya-ku, Tokyo 157-8572,
Japan, Department of Chemistry, Technion-Israel Institute of Technology, Technion City, Haifa 32000, Israel,
and Graduate School of Molecular Chemistry, Faculty of Engineering, Hokkaido University,
Sapporo 060-8628, Japan

Received: August 24, 2001; In Final Form: February 27, 2002

Intramolecular excitation energy transfer has been investigated with bichromophoric compounds in which naphthalene and anthracene as donor (D) and acceptor (A), respectively, are linked through a methylene chain, i.e., 9-anthryl-(CH₂)_n-1-naphthyl (AnN) with *n* = 1, 3, and 6 methylene units as spacer. The respective compounds were dispersed in stretched PVA films with the expectation that the methylene chain takes preferred conformations elongated in the direction of stretching polymer films so that the D–A distances are determined by the methylene chain length. From analyses of picosecond time-resolved fluorescence spectra and the fluorescence decay kinetics, it has been found that the energy transfer rates show a systematic change depending on the number of the methylene chain units: $47.6 \times 10^{10} \text{ s}^{-1}$ in A1N, $1.96 \times 10^{10} \text{ s}^{-1}$ in A3N, and $0.15 \times 10^{10} \text{ s}^{-1}$ in A6N at 10 K. These changes in the energy transfer rate are basically consistent with the theoretical estimation based on the Förster's mechanism, with some contribution from through-bond superexchange interaction. The energy transfer rates in *nonstretched* PMMA films show no systematic change and are faster than those in *stretched* PVA films, suggesting a large contribution of the folded conformers of D and A. The time-resolved fluorescence spectra of anthracene (A) moiety show an unusual profile in a short time region (<20 ps) in which the 0–0 band is less intense than the 0–1 band. The fluorescence of the anomalous profile was assigned as being due to a resonance emission from higher vibrational levels in S₁ populated by the energy transfer process.

1. Introduction

Special attention has recently been paid to the photoinduced interaction between two chromophores incorporated in a single molecule. Chromophores in such molecular systems have relatively strong interchromophore interaction, and they may undergo very fast photophysical processes such as excitation energy transfer.¹ Our recent studies on interchromophore energy transfer in highly organized molecular systems have demonstrated that the reaction time scales are less than 1 ps, which are comparable to or shorter than intramolecular relaxations such as vibrational relaxation (VR) and internal conversion (IC).² In these cases, the excitation energy transfer (EET) occurs as a nonequilibrium energy transfer from the S₂ state or vibrationally hot S₁ state of the donor before thermal equilibration. Recent experimental studies by means of time-resolved spectroscopies have revealed a significant contribution of such nonequilibrium processes to the overall ultrafast reaction dynamics.²

Several groups have investigated intramolecular EET in bichromophoric compounds containing naphthalene as the energy donor (D) and anthracene as the acceptor (A), i.e., 9-anthryl-(CH₂)_n-1-naphthyl (hereafter referred to as AnN) with *n* = 1, 3, and 6 methylene units as spacer. The structural formula of these compounds are shown in Figure 1. Schnepf and Levy³

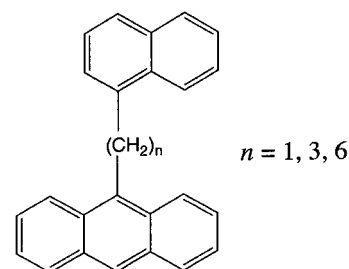


Figure 1. Molecular formula of AnN compounds.

found that, following excitation of D moiety, only anthracene fluorescence was observed irrespective of the excitation wavelength and that the intramolecular EET occurs very fast with quantum efficiencies larger than 99%. Recently, Schael et al.⁴ and Wang et al.⁵ studied it with the supersonic-jet molecular beam for A1N, A3N, and A6N and estimated the energy transfer rate to be 1.5 ps for A1N from the homogeneous line width in the absorption spectrum. They found also that A3N and A6N exhibit very fast EET similarly to A1N, indicating that these molecules take predominantly folded structures with a face-to-face conformation of D and A chromophores in a supersonic jet. This situation may probably hold in fluid solution. Indeed, the picosecond time-resolved fluorescence study by Nishimura et al.⁶ showed that AnN's in *n*-hexane solution exhibit no fluorescence emission of naphthalene (D) even in a very short time region and the transfer rate is to be less than 5 ps. Another problem in studying the EET dynamics in AnN's is that the

* To whom corresponding should be addressed. Phone: 81-11-706-6606.
Fax: 81-11-709-2037. E-mail: yamiw@eng.hokudai.ac.jp.

[†] Aoyama Gakuin University

[‡] Hokkaido University

[§] Technion-Israel Institute of Technology.

flexible bridge structure may have more or less a distribution of different bichromophore conformations in solution. Thus, the experimental results for EET are the reaction dynamics integrated over an ensemble of molecules with different D–A distances. Such experimental conditions make it difficult to examine the D–A distance dependence of EET processes in a series of AnN's.

On the other hand, Scholes et al.⁷ have examined the EET between naphthalene (D) and anthracene (A) incorporated in a rigid bis(norbornyl) bicyclo[2,2,0]hexane bridge in which D and A moieties are fixed in distance (12.24 Å) and orientation. They found that the observed EET rate is larger than that estimated from the Förster's mechanism, and proposed that a contribution from superexchange through-bond interaction is involved in the EET process in addition to the through space dipole–dipole interaction.

For AnN series of compounds (Figure 1), a special experimental technique is needed for stretching a methylene chain and separating the two end groups of D and A far apart. The method of stretched polymer film^{8,9} might be adapted for this purpose. It has been established by Hoshi and Tanizaki^{8,9} that, with polymer films such as PVA in which rodlike molecules or molecules with flexible methylene chain are dispersed, when these polymer films are stretched in one direction, rodlike molecules within the polymer films are oriented such that the longitudinal molecular axis is oriented toward the stretching direction. In the case of the flexible compounds such as AnN's, this method allows the flexible molecules to elongate in the direction of stretching. Therefore, by using this technique, one can examine the D–A distance dependence on the intramolecular EET rate much more precisely than those of fluid solution in previous studies.

In the present study, we have studied the intramolecular EET for A1N, A3N, and A6N incorporated in the stretched polymer films, with an expectation that these molecules may take preferably a conformation elongated in the stretching direction. The D–A distance dependence on the EET rate has been investigated with a picosecond time-resolved fluorescence spectroscopy at 10 K and room temperature. The relative magnitude of EET rates were compared with the theoretical values obtained from the Förster's theory for the resonance EET. Associated with the fast EET reaction, it has been found that a resonance fluorescence emitted from higher vibrational levels of A was observed. This will be discussed in relation to the vibrational relaxation in S_1 vibrational manifold of anthracene.

2. Experimental Section

Preparation of Stretched Polymer Films. The compounds A1N, A3N, and A6N were synthesized by the method previously reported.¹⁰ The polymer films were prepared from commercial poly(vinyl alcohol) (degree of polymerization = 1500) as described previously.¹¹ The PVA films of 0.13–0.18 mm thickness were immersed in a methanol solution containing the AnN compound with concentration of 1.0×10^{-3} M for 20 min. During this process, the compounds are assumed to penetrate into the films. After removal of solvent, the polymer films were stretched uniaxially as shown schematically in Figure 2. A polymer film sheet was expanded in a direction as indicated by an arrow under constant temperature (ca. 80 °C). When four points marked on a film surface with distances of a_0 and b_0 ($a_0 = b_0$) were changed to the points with distances of a_1 and b_1 upon stretching, the stretching ratio R_s was defined as $R_s = b_1/a_1$. In the present study, the PVA film was stretched as $R_s =$ ca. 5.3 in a stretching time of 30 s.

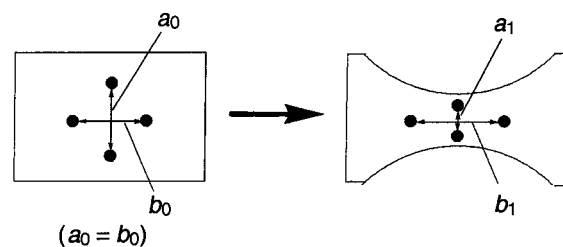


Figure 2. Schematic illustration of stretching and transformation of a PVA film. The four points are marked on a surface of a film with distances a_0 (in the y axis) and b_0 (in the x axis). When a film is stretched in a direction shown by an arrow, the ratio $S_0 = b_0/a_0$ before stretching is changed into $S_1 = b_1/a_1$. In the present study, the stretched films were prepared as $S_1 =$ ca. 5.3.

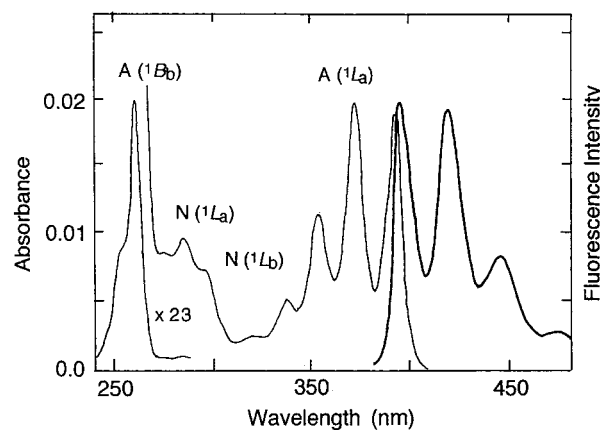


Figure 3. Absorption and fluorescence spectra of A3N in stretched PVA film at 10 K.

Time-Resolved Fluorescence Measurements. Absorption spectra and steady-state fluorescence spectra were recorded with a JASCO Ubest-50 spectrophotometer and a Hitachi F-4500 fluorescence spectrometer, respectively. Fluorescence decay curves and time-resolved fluorescence spectra were measured with a picosecond pulse laser and a single-photon timing apparatus.¹² The laser system was a mode-locked Ti:sapphire laser (Coherent, Mira 900) and pumped by an argon ion laser (Coherent, Innova 300) combined with a pulse picker (Coherent, model 9200). The third harmonics (280 nm) generated by an ultrafast harmonic system (Inrad, model 5-050) was used as an excitation light source. The decay curve was obtained by monitoring the emission with a microchannel-plate photomultiplier (Hamamatsu R2809U-01). The pulse width of the instrumental response function was 30 ps (fwhm). The picosecond time-resolved fluorescence spectra were obtained from decay curves monitored at different wavelengths ranging from 300 to 600 nm in a step of 0.625 nm. The time-resolved spectrum was constructed from a series of decay curves by plotting the fluorescence intensities at the given delay times as a function of emission wavelength.

3. Results

3.1. Absorption and Fluorescence Spectra. The absorption and fluorescence spectra of A3N in stretched polymer films at 10 K, as a representative example, is shown in Figure 3. The anthracene absorption bands of $S_0 \rightarrow S_1$ (1L_a) and $S_0 \rightarrow S_3$ (1B_b) appear in the wavelength regions of 330–400 and 250–270 nm, respectively, with well-defined vibrational structures, and the naphthalene absorption bands of $S_0 \rightarrow S_1$ (1L_b) and $S_0 \rightarrow S_2$ (1L_a) appear in wavelength regions of 310–320 and 270–300 nm, respectively. Similar spectra were obtained for A1N and

TABLE 1: Fluorescence Lifetimes and Amplitudes of Naphthalene (D) and Anthracene (A) in A1N, A3N, and A6N in Stretched PVA Films with Excitation of D at 280 nm

compound	10 K		296 K	
	obs.345 nm/ (D; ps)	obs.398 nm/ (A; ps)	obs.345 nm/ (D; ps)	obs.398 nm/ (A; ps) ^z
A1N	2.1 ^a (1.0) ^b	9165 (1.0) ^c	2.9 (1.0)	8379 (1.0) ^c
A3N	51 (0.84)	87 (−1.0)	18 (0.65)	38 (−1.0)
	173 (0.16)	10920 (1.0)	153 (0.35)	10250 (1.0)
A6N	71 (0.09)	97 (−1.0)	56 (0.18)	111 (−1.0)
	687 (0.55)	10900 (1.0)	380 (0.52)	10370 (1.0)
	4500 (0.46)		4090 (0.30)	

^a The accuracy of the measured lifetime values is ± 1.0 ps. ^b The values in parentheses are amplitudes of exponential decay components.

^c The rise component might be involved, but its rise time was not determined within the accuracy of curve-fitting analysis.

A6N. In all compounds, the absorption spectra can be described as a simple superposition of respective absorption spectra of naphthalene and anthracene.

Upon excitation of naphthalene (D) in A1N at 280 nm, a steady fluorescence spectrum gives almost exclusively the anthracene (A) spectrum. In A6N and A3N, the fluorescence intensities of naphthalene were less than 0.5% of that of anthracene, and they were too weak to be analyzed quantitatively. The fluorescence spectrum, as shown in Figure 3, shows a typical spectrum of anthracene with a well-defined vibrational structure. The spectral profiles in the absorption and fluorescence mentioned above are common to A1N and A6N. At 296 K, the bandwidth of the respective vibrational bands are somewhat broader than those at 10 K.

3.2. Fluorescence Decay Curve Analysis. Table 1 summarizes the results of the analysis for the fluorescence decay curves upon excitation at 280 nm (naphthalene, D) in *stretched* PVA films. The decay curve of D fluorescence in A1N is almost single exponential with a very short lifetime at 10 and 296 K, whereas those in A3N and A6N are composed of two or three exponential decay functions with short and long lifetimes. By taking into consideration a decay component with the dominant amplitude in every case of AnN's, one can see a striking feature of the decay kinetics, particularly at 10 K, namely, that the lifetime changes systematically on going from A1N to A6N. The lifetime becomes longer with increasing the number of the methylene chain unit: 2.1 ps in A1N, 51 ps in A3N, and 687 ps in A6N. The complicated decay curves of D in A3N and A6N indicate that there still exists a conformational distribution of flexible molecules which gives a distribution of the energy transfer rate even in stretched films. The decay curves of anthracene (A) fluorescence are described simply by a single-exponential rise and decay.

In the decay curves of anthracene (A) fluorescence at 10 and 296 K, the rise components give the time constants which are not consistent with the decay times of the corresponding donor. The primary reason for this inconsistency comes from difficulties in the curve-fitting analyses for the curves involving fast rise and slowly decaying components, and the curve-fitting analyses suffer from uncertainty in extracting a fast rise component. The decay constants of A (10–12 ns) are corresponding to the intrinsic anthracene decay. The fluorescence lifetimes of 9-methylanthracene in PMMA films gave 12.5 ns at 10 K and 9.2 ns at 296 K.

At 296 K, the decay curves of D on the whole exhibit fairly faster decay kinetics relative to those at 10 K. This is consistent with only a weaker appearance of D fluorescence in the time-resolved spectra in the short time region as discussed in the

TABLE 2: Fluorescence Lifetimes and Amplitudes of Naphthalene (D) and Anthracene (A) in A1N, A3N, and A6N in Nonstretched PMMA Films with Excitation of D at 280 nm

compound	10 K		296 K	
	obs.345 nm/ (D; ps)	obs.398 nm/ (A; ps)	obs.345 nm/ (D; ps)	obs.398 nm/ (A; ps)
A1N	3.5 (1.0) ^a	15 (−1.0)	2.7 (1.0)	14 (−1.0)
		12000 (1.0)		11000 (1.0)
A3N	19 (0.58)	14 (−1.0)	14 (0.74)	16 (−1.0)
	197 (0.42)	12000 (1.0)	140 (0.26)	9300 (1.0)
A6N	37 (0.50)	51 (−1.0)	46 (0.63)	80 (−1.0)
	188 (0.41)	11000 (1.0)	148 (0.32)	11000 (1.0)
	3800 (0.09)		3100 (0.05)	

^a The values in parentheses are amplitudes of exponential decay components.

next section. In A1N, the decay kinetics at 296 K are almost the same as that at 10 K, whereas in A3N and A6N, the fast decay is involved with substantial amplitudes. This complexity in A3N and A6N is probably a consequence of formation of folded conformers at room temperature in stretched films.

Table 2 summarizes the fluorescence lifetimes for A1N, A3N, and A6N in *nonstretched* PMMA films at 10 and 296 K. All of the decay curves can be analyzed phenomenologically in the same way as in the stretched films. In striking contrast to the case of stretched films, the decay kinetics are determined by the faster decays, and as for the component with the dominant amplitude, the decay properties show no systematic change on going from A1N to A6N. It then follows that AnN's in *nonstretched* films have a broader distribution of folded conformers, resulting in faster decay kinetics.

3.3. Time-Resolved Fluorescence Spectra of AnN in Stretched PVA Films. Figure 4 shows time-resolved fluorescence spectra of A1N, A3N, and A6N in stretched PVA films at 10 K, obtained with a pulsed laser excitation at 280 nm (naphthalene, D). In every case, both of the fluorescence emissions of D and A appear in the spectra of a short time region before 100 ps: the naphthalene fluorescence at 300–400 nm and the anthracene fluorescence at 400–500 nm. The intensity of D fluorescence becomes stronger in order of A1N, A3N, and A6N. This trend in D fluorescence intensity is qualitatively in accord with the change in fluorescence lifetime mentioned in the preceding section. Because the intensity of D fluorescence reflects the EET rate and therefore related to the D–A distance, a systematic change in the D spectra indicates that the D and A moieties are preferably far apart in the stretched film and that the intramolecular EET occurs with the reaction rate depending on the methylene chain length and the D–A distance.

One should note that the spectral profile of anthracene (A) in respective AnN compounds changes with time (Figure 4): the spectrum at earlier time (0–20 ps) is significantly diffuse, and the intensity ratio of the vibrational bands (0–0) and (0–1) is reversed relative to the ordinary anthracene spectrum, whereas in the later time region, the spectrum has an ordinary profile as shown in Figure 3. The diffuseness in the earlier spectra is pronounced in A1N. Furthermore, it is found from detailed analyses of the spectra that the vibrational band shifts with time; the 0–0 band locates at 404 nm at 0 ps, but after 50 ps, it does shift to 396 nm. The plots of the peak wavelengths at 10 K will be presented in the Discussion section. At 296 K, the naphthalene (D) spectrum also appears in a short time region, but its intensity is much weaker than those at 10 K. This might be accounted for by the faster energy transfer at 296 K than at 10 K. The intensity of D fluorescence increases in the order of

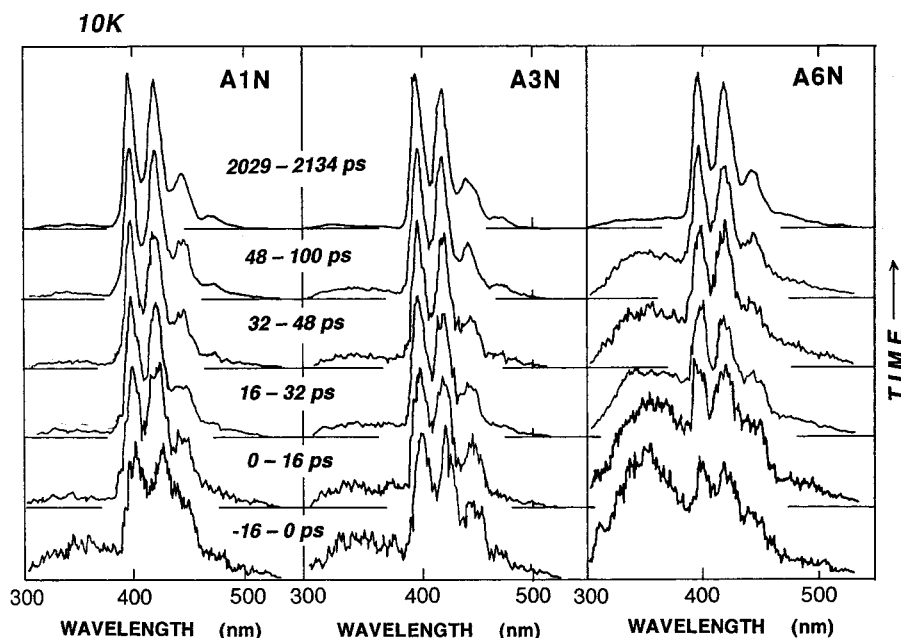


Figure 4. Time-resolved fluorescence spectra of A1N, A3N, and A6N in stretched PVA films at 10 K. The excitation wavelength is 280 nm (1L_a absorption band of naphthalene).

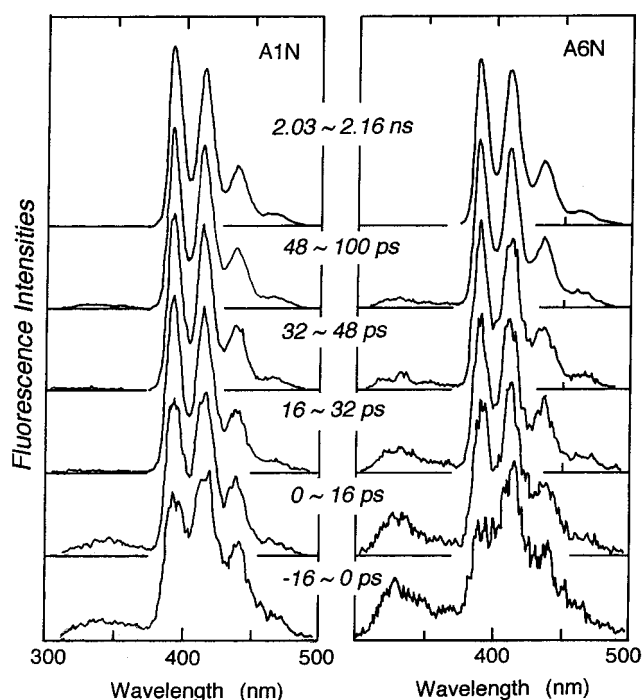


Figure 5. Time-resolved fluorescence spectra of A1N and A6N in nonstretched PMMA films at 10 K. The excitation wavelength is 280 nm (1L_a absorption band of naphthalene).

A1N, A3N, and A6N. The spectral diffuseness and peak shift are also seen at room temperature, but the changes into an ordinary spectrum occur much faster within 10 ps. Overall the rate of appearance of the anthracene moiety fluorescence band is a direct measure of the intramolecular EET rate.

3.4. Time-Resolved Fluorescence Spectra of AnN and 9-Methylanthracene in Nonstretched PMMA Films. Figure 5 shows the time-resolved fluorescence spectra for A1N and A6N in *nonstretched* PMMA films at 10 K. In comparison with the corresponding spectra of *stretched* PVA films (Figure 4), it is seen that the naphthalene (D) fluorescence is very weak, and the anthracene (A) spectrum has an unusual and diffuse spectral

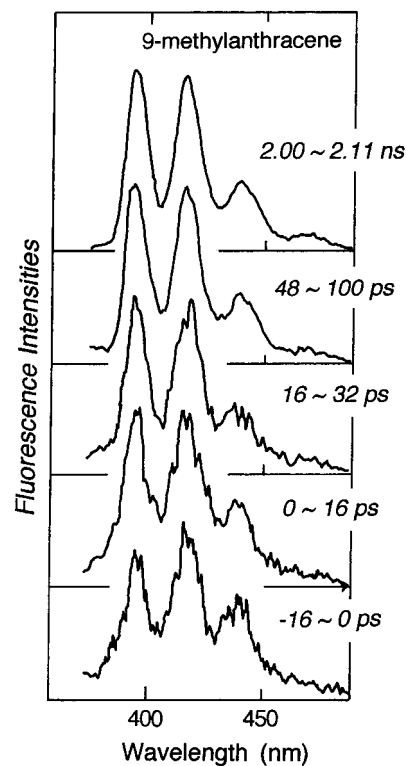


Figure 6. Time-resolved fluorescence spectra of 9-methylanthracene in nonstretched PMMA films at 10 K. The excitation wavelength is 280 nm.

features with a weaker 0–0 band relative to the 0–1 band. The unusual spectrum evolves into the normal spectrum of anthracene after 30 ps. It appears that the weak intensity of D fluorescence in nonstretched films conforms with the short fluorescence lifetime of D (Table 2).

Figure 6 shows the time-resolved fluorescence spectra of 9-methylanthracene in nonstretched PMMA film at 10 K, measured with a laser excitation at 260 nm (1B_b). The spectrum changes with time similarly to those of AnN series. In an earlier time, the spectrum has a profile with the 0–1 band intensity

being higher than the 0–0 band intensity. After 10 ps, it changes into the normal spectrum. The fluorescence spectrum taken by excitation at $S_0 \rightarrow S_1$ (1L_a) absorption band does not change throughout the time range and is essentially identical to the normal spectrum.

4. Discussion

The present experimental results for the intramolecular EET in A1N, A3N, and A6N in *stretched* PVA films can be summarized as follows: (1) The time-resolved fluorescence spectra exhibit D fluorescence in a short time region less than 100 ps at 10 K. The intensity of D fluorescence increases on going from A1N to A6N. (2) For the dominant decay component of the fluorescence at 10 K, the lifetime value increases in the order of increasing methylene chain length. (3) The anthracene (A) moiety fluorescence at the short time region of less than 20 ps is somewhat different from the well-known spectrum of A in the observed intensity ratio of the 0–0 to 1–0 bands. We will discuss points 1 and 2 in the light of the effect of stretched polymer films on the molecular orientation and elongation of methylene chains in order to obtain a conclusive picture of the D–A distance dependence of the intramolecular EET rate. Finally, we will discuss point 3 in terms of the vibrational relaxation process from higher vibrational levels of anthracene S_1 state populated through EET.

4.1. Conformational Distribution of A1N, A3N, and A6N.

The flexible polymethylene chains incorporated as molecular spacers allow the AnN-type molecule to take a number of different conformations by rotation of every C–C single bond in methylene chain. Therefore, the AnN molecules dispersed in fluid solution or polymer films should be described basically by an ensemble of different conformers with different D–A distances and mutual orientations. Speiser et al.^{4,5} examined the probability distribution of possible conformations with the computational simulation for a series of AnN's in the gas phase. The computer simulation predicted that the conformational distributions for A1N and A3N are narrow, and only few conformations exhibit significant Boltzmann factors, whereas that for A6N is broader and exhibits several maxima. For A3N and A6N, the most stable conformation exhibits a sandwich-like orientation of the chromophore units, whereas in A1N, the single methylene group is not flexible enough to allow the two chromophores to attain close proximity. The D–A distances r_{DA} in these most stable conformations are 3.3 Å in A3N, 3.8 Å in A6N, and 4.3 Å in A1N. It is worth noting that r_{DA} falls between ca. 3 and 5 Å despite the fact that the flexibility of the methylene chain allows distances up to 7.7 Å in A3N and 11.6 Å in A6N, and that A3N and A6N take similar structures with a folded conformation. The association of the end groups was interpreted in the force field simulation by assuming the energy gain of ca. 7 kcal/mol from attractive forces between the two chromophores.¹³

Thus, the previous experimental results for intramolecular EET in AnN's in solution and supersonic jet expansion are reasonably explained in conformity with the simulation results. The A3N and A6N compounds commonly tend to have folded conformers resulting in very fast energy transfer (rate constant $k_{ET} > 1 \times 10^{11} \text{ s}^{-1}$) between closely stacking D and A moieties. Although A1N cannot take a folded conformer, the energy transfer rate is basically fast because of the short distance of D–A. On the other hand, in the stretched polymer films used in the present study, AnN's are expected to take the stretched conformations in which the methylene chain is elongated in one direction and the D and A moieties are separated with the largest

distance. This supposition will be actually evidenced from the reaction kinetics as discussed in the following section.

4.2. Energy Transfer Rates and Conformation of AnN's in Stretched PVA Films. The fluorescence lifetime of D is connected directly to the rate of intramolecular EET, as shown below, which allows one to investigate the D–A distance dependence of the EET rate and the mechanism of EET. The lifetime value in *stretched* films at 10 K (Table 1) changes systematically in the order of the methylene chain length; for the decay component of dominant amplitude, $\tau_F = 2.1, 51,$ and 687 ps for A1N, A3N, and A6N, respectively. On the other hand, in *nonstretched* films, the fluorescence lifetimes (Table 2) show no such systematic change on going from A1N to A6N, and the short decay components of $\tau_F = 20\sim 50 \text{ ps}$ are involved in the decays of A3N and A6N with large amplitudes. It follows that the respective compounds in *stretched* films take predominantly a stretched conformer with the D–A distance far apart, whereas those in *nonstretched* films have broader distribution of conformation with a larger contribution of folded and sandwich-like conformations, similar to the observation made in solution.⁶ This difference between *stretched* and *nonstretched* films is recognized obviously as being due to an effect of stretching the film and elongating the molecules. One should note here that the conformation distribution in stretched films depends on temperature. As is seen in Table 1, the change of lifetime of D on going from A1N to A6N is less systematic at 296 K than at 10 K. Particularly, larger amplitudes of the fast decay in A3N and A6N at 296 K indicate a larger contribution of the folded structure at room temperature.

For this reason, we confine our discussion to the EET dynamics associated with the fluorescence decays with the dominant amplitude in the stretched film at 10 K, which will correlate directly with the D–A distance dependence on the EET rate for the AnN molecules. The fluorescence lifetime (τ_F) is related to the energy transfer rate (k_{ET}) by

$$\tau_F = \frac{1}{k_F + k_{ET}} \approx \frac{1}{k_{ET}} \quad (1)$$

where $k_F = (\tau_F^0)^{-1}$ with τ_F^0 representing the fluorescence lifetime of a reference molecule without an anthracene moiety. In this study, we use the lifetime value of 1-methylnaphthalene; that is, $\tau_F^0 = 70 \text{ ns}$ in PMMA film at 10 K. Then the k_{ET} values are calculated to be $47.6 \times 10^{10} \text{ s}^{-1}$ in A1N, $1.96 \times 10^{10} \text{ s}^{-1}$ in A3N, and $0.145 \times 10^{10} \text{ s}^{-1}$ in A6N in stretched PVA films at 10 K.

According to the Förster's mechanism of energy transfer due to the dipole–dipole interaction, the EET rate constant is expressed by the following equation:

$$k_{ET} = \left(\frac{R_0}{R} \right) \frac{1}{\tau_F^0} \quad (2)$$

where R_0 is the Förster's critical energy transfer distance denoted as

$$R_0 = \frac{9000\kappa^2\Phi_F \ln 10}{128\pi^5 n^4 N R^6} \int \frac{f_D(\nu)\epsilon_A(\nu)}{\nu^4} d\nu \quad (3)$$

where ν is wavenumber of fluorescence, $\epsilon_A(\nu)$ is the molar extinction coefficient, $f_D(\nu)$ is the normalized spectral distribution of donor fluorescence, N is Avogadro's number, Φ_F is the fluorescence quantum yield of donor, n is refractive index of solvent, and R is the center-to-center distance of A and D. The

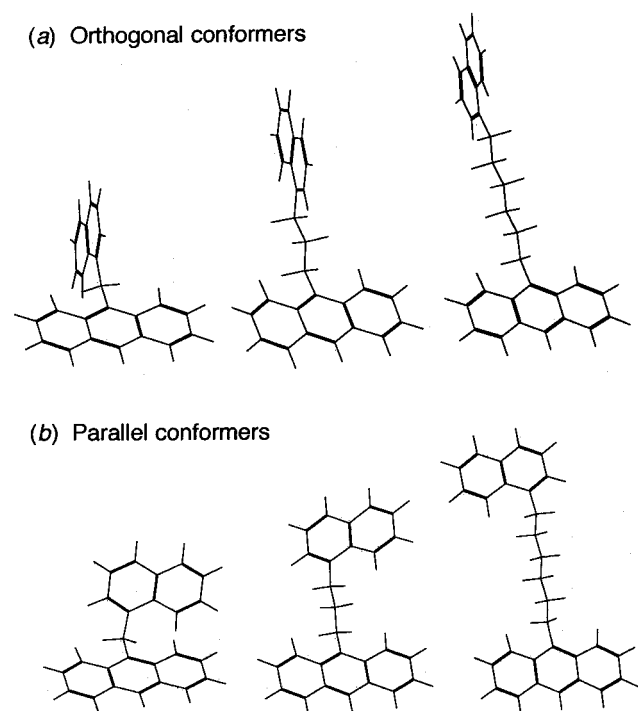


Figure 7. Two types of stretched conformers with orthogonal (a) and parallel (b) orientations of the two end groups of D and A chromophores for A1N, A3N, and A6N.

orientation factor κ , is expressed as

$$\kappa = \cos \phi_{DA} - 3 \cos \phi_D \cos \phi_A \quad (4)$$

where ϕ_{DA} is the angle between the transition dipole moments of D and A and ϕ_D and ϕ_A are the angles between the respective transition moments and the distance vector \mathbf{R} . The transition dipole moment of $S_0 \rightarrow S_1$ (1L_b) transition in naphthalene (D) is in the short molecular axis, whereas that of anthracene (A) (1L_a) is in the long molecular axis. The k_{EET} values were calculated by using the literature value $R_0 = 25.51 \text{ \AA}$ for 1-methylnaphthalene (D) and anthracene (A).¹⁴

Taking into consideration that there still exist possible conformers with respect to mutual orientation of the two end groups in stretched films, we calculated for the two extremes of conformations that the molecular planes of D and A are parallel and perpendicular. These possible two conformers are shown in Figure 7. The actual conformations are supposed to take either parallel or perpendicular conformation or to be distributed between these two extremes. The results of calculation are summarized in Table 3. It is seen that the calculated k_{EET} values are in fair agreement with the corresponding experimental values. In cases of A3N and A6N, the experimental values fall between the values for the two conformers, $(0.02 \sim 1.8) \times 10^{10} \text{ s}^{-1}$. Particularly, in A3N, the EET rate for the orthogonal conformer of A3N coincides with the experimental value within the limits of experimental error, and in A6N, it is in an intermediate between the two conformers. This may suggest that A3N assumes the orthogonal conformation preferably to the parallel conformer, whereas A6N exists as a mixture of the two conformers. In A1N, the calculated k_{EET} value is one-half of the experimental value; however, at such short interchromophore separations, Förster formulation, which is valid only for point dipoles, gives only a rough estimate of the correct EET rate. Moreover, at these distances, one has to take into account an exchange interaction due to orbital overlap.¹ Note that, Scholes et al.⁷ found that the intramolecular EET in

a bichromophoric compound consisting of naphthalene and anthracene connected through a norbornyl bridge is faster than the rate estimated from the Förster's dipole–dipole interaction and proposed a contribution from a through-bond interaction in addition to the Förster-type through-space interaction. In the present case of A1N, a contribution from the similar through-bond interaction via a single methylene group is probably responsible for the EET rate larger than the calculated one.

Besides the dominant component in the fluorescence decays, the slow components that appeared in A6N at 10 and 296 K exhibit 4.1–4.5 ns lifetimes with fairly large amplitudes (Table 1). These values give the k_{EET} values of $(0.022 \sim 0.024) \times 10^{10} \text{ s}^{-1}$ which are consistent with the calculated k_{EET} values for the parallel conformation ($0.022 \times 10^{10} \text{ s}^{-1}$) as shown in Table 3. It follows that the in A6N the parallel conformation may possibly be involved in the conformation distribution in stretched films in addition to the orthogonal conformation.

In conclusion, the AnN's molecules incorporated in stretched films prefer a conformation in which the methylene chain is elongated and the two end groups of D and A are separated far apart. For this conformation, the intramolecular EET in AnN's on the whole can be described approximately in terms of the Förster's dipole–dipole interaction mechanism, with some contributions from through-space exchange and through-bond superexchange interactions. On the other hand, the nonstretched films exhibit an EET rate which is much faster than that of the stretched films, indicating that A3N and A6N in films take predominantly folded conformations similar to the cases of AnN's in fluid solution.

4.3. Fluorescence Spectral Change and Peak Shift: Vibrational Relaxation in the Excited State of Anthracene. The time-resolved fluorescence spectra of A1N, A3N, and A6N (Figure 4) show that the spectra at 0–20 ps exhibit an unusual profile different from that of the ordinary vibrationally relaxed spectrum of anthracene. In comparison with the anthracene spectrum, the spectrum is significantly diffuse, the intensity of 0–0 band is lower than that of 0–1 band, and the band maxima of 0–0 and 0–1 shift 4–6 nm to the red. Figure 8 shows plots of the wavelength of the 0–0 band as a function of time for A1N, A3N, and A6N. It is seen that in every case the 0–0 band is shifted from 404 to 396 nm during the first 60 ps, and it reaches a constant wavelength value after 60 ps which is the same wavelength as in the steady-state fluorescence spectra. Similar time behaviors of spectral profile and peak shift were observed in 9-methylanthracene (9-MA) in PMMA film when the molecules are excited at 260 nm (1B_b). However, for excitation at $S_0 \rightarrow S_1$ (1L_a), no such changes are seen throughout the time range. The spectral change in 9-MA occurs within 20 ps. One should note that these time evolutions of the spectrum are usually associated with excitation onto higher vibrational levels in the S_1 state. This is the case with the excitation of the anthracene moiety through the EET process from an excited naphthalene in AnN's and also for direct optical excitation of methylanthracene.

We assign the unusual fluorescence spectrum of A appearing during the first 20 ps as being due to a resonance fluorescence emission (RF) from higher vibrational levels of the S_1 state of the anthracene moiety. The relaxation processes of excitation energy in AnN's are illustrated in Figure 9. Following excitation of the naphthalene (D) moiety into the S_2 state, the excited naphthalene undergoes rapid internal conversion $S_2 \rightarrow S_1$ (probably within 0.1 ps), followed by EET to anthracene which occurs on the time scale of 2–10 ps corresponding to the fast fluorescence decay component. This is followed by fluorescence

TABLE 3: Calculated Förster Energy Transfer Rates for the Two Conformers with Orthogonal and Parallel Orientations for the Two End Groups of D and A as Shown in Figure 7

compound	orthogonal conformation			parallel conformation			k_{EET} (exptl) (10^{10} s^{-1})
	R^a (Å)	κ^2^b	k_{EET} (10^{10} s^{-1})	R (Å)	κ^2	k_{EET} (10^{10} s^{-1})	
A1N	5.56	1.09	21.8 (1.00) ^c	4.96	0.57	22.5 (1.03)	47.6 (2.18)
A3N	8.18	0.90	1.77 (0.08)	7.60	0.32	0.98 (0.04)	1.96 (0.09)
A6N	11.90	1.42	0.29 (0.01)	11.70	0.098	0.022 (0.001)	0.145 (0.006)

^a The center-to-center distance between the two end groups, naphthalene, and anthracene chromophores. ^b The orientation factor in the Förster's mechanism of energy transfer. See eq 4 in text. ^c The values in parentheses are relative values normalized with the value for A1N in orthogonal conformation.

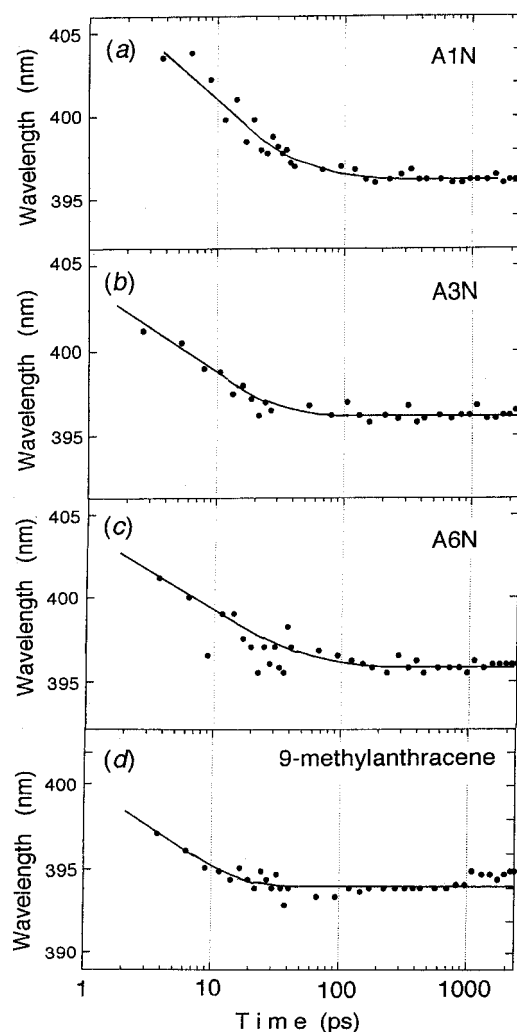


Figure 8. (a–c) Plots of wavelength of the fluorescence 0–1 band as a function of time taken from the time-resolved fluorescence spectra in stretched PVA films at 10 K for AnN. (d) Corresponding plots for 9-methylanthracene in PMMA film at 10 K.

transition from higher vibrational levels of excited anthracene ($\sim 5700 \text{ cm}^{-1}$ vibrational excess energy), competing with the vibrational relaxation (VR) in anthracene S_1 . The resonance emission should have a spectral profile different from that of the ordinary, thermally equilibrated emission because of different Franck–Condon factors. Furthermore, if the potential curve is shallower in S_1 relative to that in S_0 , corresponding vibrational bands should be blue-shifted as the VR process goes on. This picture of the resonance fluorescence is strongly supported from comparison with the fluorescence spectrum in anthracene vapor (1.1 Torr) at 184 °C reported by Haebig,¹⁵ which was obtained with collective excitation of vibrationally excited levels involved in a broad continuous band around the 1–0 absorption band. The resonance fluorescence spectrum of vapor has intensities

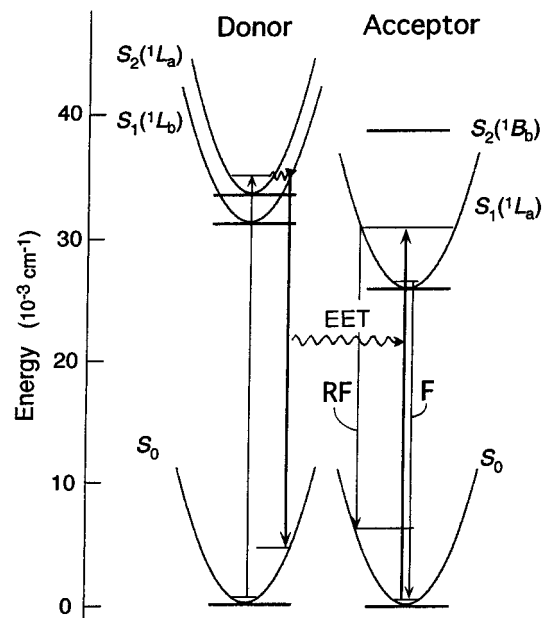


Figure 9. Energy relaxation and energy transfer processes depicted on potential curves of naphthalene (D) and anthracene (A). F represents the fluorescence thermally equilibrated, and RF represents the resonance fluorescence.

of the 0–0 band lower than that of the 0–1 band and exhibits an overall profile very similar to the one observed in the present study. Thus, the time evolution of the spectrum during the first 20 ps is to be associated with the VR process in S_1 . At room temperature, the spectral change also appears, but it is much smaller and faster than at 10 K. This means that VR is significantly faster at 296 K than at 10 K.

The net time scale of VR in the S_1 anthracene can only be estimated to be 1–2 ps, because the deduced time scales of the spectral change are resulting from convolution of the lifetime of excited naphthalene (D) under the EET process and of the excitation pulse width (30 ps). The time scales of VR in S_1 have recently been reported for several organic molecules in solution; 0.6 ps in porphyrin (THF),² 0.25 ps in azobenzene (*n*-hexane),¹⁶ and 30 ps in perylene (alkane).¹⁷ The present data for VR in anthracene provides additional data on the vibrational relaxation of organic molecules in condensed media.

Acknowledgment. We are grateful to Professor M. B. Rubin for supplying the AnN compounds. The present work is supported by a Grant-in-Aid for Scientific Research on Priority Areas (B) (No. 11223203) from the ministry of Education, Science, Sports, and Culture of Japan. S.S. acknowledges support from the VPR fund and form the Fund for the Promotion of Research at the Technion.

References and Notes

- (1) Speiser, A. *Chem. Rev.* **1996**, 96, 1953.

- (2) Yamazaki, I.; Akimoto, S.; Yamazaki, T.; Shiratori, H.; Osuka, A. *Acta Phys. Polonica A*, **1999**, 95, 105. Akimoto, S.; Yamazaki, T.; Yamazaki, I.; Nakano, A.; Osuka, A. *Pure Appl. Chem.* **1999**, 71, 2107.
- (3) Schnepf, O.; Levy, M. *J. Am. Chem. Soc.* **1962**, 84, 172.
- (4) Schael, F.; Rubin, M. B.; Speiser, S. *J. Photochem. Photobiol. A: Chem.* **1998**, 115, 99.
- (5) Wang, X.; Levy, D. H.; Rubin, M. B.; Speiser, S. *J. Phys. Chem. A* **2000**, 104, 6558.
- (6) Nishimura, Y.; Yasuda, A.; Speiser, S.; Yamazaki, I. *Chem. Phys. Lett.* **2000**, 323, 117.
- (7) Scholes, G. D.; Ghiggino, K. P.; Oliver, A. M.; Paddon-Row, M. N. *J. Phys. Chem.* **1993**, 97, 11871.
- (8) Hoshi, T.; Tanizaki, T. *Z. Phys. Chem. Neue Folge* **1970**, 230, 71.
- (9) Hoshi, T.; Kobayashi, M.; Yoshino, J.; Komuro, M.; Tanizaki, Y. *Ber. Bunsen-Ges. Phys. Chem.* **1979**, 83, 821.
- (10) Rona, P.; Feldman, U. *J. Chem. Soc.* **1958**, 1737.
- (11) Ito, T.; Higuchi, J.; Hoshi, T. *Chem. Phys. Lett.* **1975**, 35, 141.
- (12) Ohta, N.; Tamai, T.; Kuroda, T.; Yamazaki, T.; Nishimura, Y.; Yamazaki, I. *Chem. Phys.* **1993**, 177, 591.
- (13) Lal, M.; Spencer, D. *Mol. Phys.* **1971**, 22, 649.
- (14) Berlman, I. B.; *Energy Transfer Parameters of Aromatic Compounds*; Academic Press: New York, 1973.
- (15) Haebig, J. E. *J. Mol. Spectrosc.* **1968**, 25, 117.
- (16) Azuma, J.; Tamai, N.; Shishido, A.; Ikeda, T. *Chem. Phys. Lett.* **1998**, 288, 77.
- (17) Jiang, Y.; Blanchard, G. J. *J. Phys. Chem.* **1994**, 98, 9417.